Journal of Molecular Graphics and Modelling 28 (2009) 330–335

Contents lists available at ScienceDirect

Journal of Molecular Graphics and Modelling

journal homepage: www.elsevier.com/locate/JMGM

Molecular docking of a series of peptidomimetics in the trypanothione binding site of *T. cruzi* Trypanothione Reductase

Samuel Silva da Rocha Pita [a,*], José Jair Vianna Cirino [a,1], Ricardo Bicca de Alencastro [a,2], Helena Carla Castro [b], Carlos Rangel Rodrigues [c], Magaly Girão Albuquerque [a,**]

[a] *Universidade Federal do Rio de Janeiro (UFRJ), Instituto de Química, Laboratório de Modelagem Molecular (LabMMol), Cidade Universitária, Ilha do Fundão, Centro de Tecnologia, Bloco A, 6º Andar, Sala 619, Rio de Janeiro, CEP 21941-909, RJ, Brazil*

[b] *Universidade Federal Fluminense (UFF), Instituto de Biologia, Departamento de Biologia Celular e Molecular, Laboratório de Antibióticos, Bioquímica e Modelagem Molecular (LABioMol), Niterói, CEP 24210-130, RJ, Brazil*

[c] *Universidade Federal do Rio de Janeiro (UFRJ), Faculdade de Farmácia, Departamento de Medicamentos, Laboratório de Modelagem Molecular e QSAR (ModMolQSAR), Rio de Janeiro, CEP 21941-590, RJ, Brazil*

ARTICLE INFO

Article history:
Received 30 July 2009
Received in revised form 21 August 2009
Accepted 24 August 2009
Available online 31 August 2009

Keywords:
Peptidomimetic
Docking
Trypanothione Reductase
FlexX
Chagas' disease

ABSTRACT

Chagas' disease (CD) has been responsible for many deaths and disabilities mainly in South America. Currently, 40 million people are at risk of acquiring this disease and, existing therapies are still unsatisfactory, presenting harsh side effects. Therefore, the development of new chemical entities to reverse this state is critical. A series of peptidomimetics, developed by Mc Kie et al. (2001) [11], showed a reversible and competitive inhibition against *Trypanosoma cruzi* Trypanothione Reductase (TR). These inhibitors may be used as basis of lead compounds in the design of new drug candidates for the treatment of CD. In this work, we have docked this series of peptidomimetics into the TR binding site, using the FlexX algorithm as implemented in the Sybyl program, in order to access the binding mode of this class of compounds in the target enzyme.

Published by Elsevier Inc.

1. Introduction

Spread over many countries from Southern United States of America to Argentina, Chagas' disease (CD) affects about 18 million of people [1]. This endemic zoonosis is caused by the flagellated protozoan *Trypanosoma cruzi* (*T. cruzi*), which causes 21 000 deaths every year [2]. There have been many efforts to control this illness but until now the therapy based only in two drugs (nifurtimox and benznidazole) is to be replaced by a better alternative.

In 1985, Fairlamb et al. [3] reported a substrate, similar to human glutathione (GSSG), in a class of parasites (*Trypanosoma* and *Leishmania* genera) and named it as trypanothione (N1,N8-bis(glutathionyl)spermidine, TS_2). The enzyme that metabolizes this compound was named Trypanothione Reductase (TR) and has been extensively studied [4–7] as a potential target in the drug development against CD because of being a key enzyme in the *T. cruzi* redox metabolism and its absence in the human counterpart. Thus, TR had several different compounds tested against it [8–12].

Targeted allele disruption studies were unsuccessful in knocking down the TR gene in Leishmania [13,14] and some enzymatic assays concluded that in order to induce phenotypic changes in TR, compounds should have achieved 90% level of enzyme inhibition [15,16] reinforcing the essential role of this enzyme in surveillance of the parasite.

It has already been shown that a series of 21 peptides and peptidomimetics (compounds **1**–**21**, Table 1) proved to be reversible inhibitors of TR [11], and the most potent compound (**18**) showed inhibitory potency at micro-molar concentration (IC_{50} = 2.4 μM) [11]. The major advantage of this class of compounds is the feasibility of using this scaffold in a posterior schematic synthesis (e.g., combinatorial chemistry) to produce higher active compounds [17].

Using this series of compounds [11] and the crystallographic structure of TR complexed with TS_2 (natural substrate) [17], available in the Protein Data Bank [18] (PDB ID: **1BZL**), we studied by automatic docking (FlexX program) the putative binding mode

Abbreviations: CD, Chagas' disease; TR, Trypanothione Reductase; GSSG, human glutathione; N1,N8-Bis(glutathionyl)spermidine, trypanothione or TS_2.

* Corresponding author. Current address: LMDM-IBCCF/UFRJ, Brazil. Tel.: +55 21 2562 7132; fax: +55 21 2562 7132.

** Corresponding author. Tel.: +55 21 2562 7132; fax: +55 21 2562 7132.

E-mail addresses: samuelpita@iq.ufrj.br, samuelpita@biof.ufrj.br (S.S. da Rocha Pita), jjvcirino@netscape.net (J.J.V. Cirino), bicca@iq.ufrj.br (R.B. de Alencastro), hcastrorangel@yahoo.com.br (H.C. Castro), rangel@pharma.ufrj.br (C.R. Rodrigues), magaly@iq.ufrj.br (M.G. Albuquerque).

[1] Current address: CENPES/PETROBRAS, Brazil.

[2] Tel.: +55 21 2562 7132; fax: +55 21 2562 7132.

1093-3263/$ – see front matter. Published by Elsevier Inc.
doi:10.1016/j.jmgm.2009.08.011

Table 1
Structures, numbering and pIC_{50} (M) values of the 21 compounds tested against TR of *T. cruzi* (Mc Kie et al. [11]).

#	Peptides and peptidomimetics structures	pIC_{50}
1	Benzoyl-Arg-*p*-nitroanilide	3.26
2	Benzyloxycarbonyl-Arg-*p*-nitroanilide	3.40
3	H-Arg-β-naphtylamide	2.82
4	H-Trp-β-naphtylamide	2.57
5	Benzyloxycarbonyl-Lys-4-methoxy-β-naphtylamide	3.09
6	H-Trp-OH (tryptophan amino acid)	2.57
7	Benzyloxycarbonyl-Arg-Arg-4-methoxy-β-naphtylamide	4.41
8	Benzyloxycarbonyl-Arg-Arg-*p*-nitroanilide	4.22
9	H-His-Trp-His-OH	2.76
10	H-His-Trp-Lys-OH	2.41
11	H-Phe-Arg-Trp-OH	3.40
12	H-Phe-Pro-Arg-4-methoxy-β-naphtylamide	3.26
13	Benzoyl-Leu-Arg-Arg-β-naphtylamide	4.93
14	*tert*-Butyl-Leu-Arg-Arg-7-amide-methylcoumarin	3.45
15	*tert*-Butyl-Leu-Lys-Arg-7-amide-methylcoumarin	3.38
16	Benzoyl-Gly-Arg-Arg-Leu-β-naphtylamide	3.29
17	Benzyloxycarbonyl-Gly-Gly-Arg-7-amide-methylcoumarin	3.53
18	Benzyloxycarbonyl-Ala-Arg-Arg-4-methoxy-β-naphtylamide	4.98
19	Benzoyl-Lys-Phe-Arg-*p*-nitroanilide	3.62
20	Benzoyl-Phe-Val-Arg-7-amide-4-methylcoumarin	3.61
21	H-Phe-Met-Arg-Phe-NH_2	2.56

of these ligands into the active site of TR, intending to ascertain helpful and valuable clues for the design of new inhibitors. The results pinpointed not only the putative binding mode of these peptidomimetics, but also the alternative sub-pockets that could be accessed by new and more potent inhibitors of this precursor generation.

2. Materials and methods

The docking analysis was carried out using the FlexX module, a fully automatic docking tool for flexible ligands, available on Sybyl 7.0 package [19], running on CPU Intel(R) Xeon CPU 3.06 GHz, RAM Memory 2 GB, under the OS Enterprise Linux 3.0. The FlexX docking program is an automated method for posing ligands into protein binding sites [20]. This algorithm anchors a pre-selected compound fragment into a region of the protein defined by the user, and then, the remaining fragments are subsequently added to the initial fragment. When the entire structure is completed, the binding energy is estimated, and a score function is applied [20].

The crystallographic structure of the *T. cruzi* Trypanothione Reductase in complex with trypanothione (resolution of 1.6 Å) used in this study was retrieved from PDB [18] under code **1BZL** [17]. This structure was chosen since it is the only *T. cruzi* TR that contains the natural substrate at higher resolution than other earliest structures deposited at PDB. The hydrogen atoms were automatically added to the protein and formal charges were calculated using the Sybyl program. Cysteine residues 53 and 58 were corrected from cystine (Cys-S-H) form to cysteine (Cys-S-S-Cys) for all docking calculations. The FlexX docking program automatically ignores water molecules, ligands, and cofactors from the protein structure [20].

The TR natural substrate (TS_2) was re-docked into the TR binding site in order to check the accuracy of the FlexX program. The TS_2 coordinates were extracted from the original PDB file (**1BZL**), hydrogen atoms were added, partial atomic charges were assigned by Gasteiger–Hückel method and the remaining structure was optimized by the Tripos Force Field using the conjugated gradient method until the gradient convergence reached 0.05 kcal mol^{-1}. The distance dependent dielectric function was used ($\varepsilon = 3.00$) within a cut-off of 10.00 Å.

The structures of the 21 peptidomimetics were obtained from the original reference [11] and their 3D structures were built into the Sybyl program. The same protocol used for TS_2 was applied for the peptidomimetics when preparing these ligands. Amine, guanidine, and carboxylic groups were assumed to be in the ionic form at physiological pH.

Four binding site models were then defined for each docking run for all ligands (the TS_2 and the 21 peptidomimetics). The first one, named **All** binding site model, was defined as a sphere within 8.2 Å radii from the bound TS_2 molecule. This length radius is the minimum value that was able to include all ligands in a previous docking tentative. The other three binding site models were defined considering the same binding site size (8.2 Å), but, in order to inspect alternative binding modes in the enzyme, we focused on three different sub-pockets **W22**, **F396′** (′ means that this residue belongs to chain B), and **Y111**. For each residue, we assigned a sphere within 3.1 Å radii (i.e., twice the C_{sp3}–C_{sp3} bond length), which accounts for hydrophobic interaction according to Privalov and Gill [21].

Therefore, we have performed four docking runs using the 21 compounds into the same run, considering the four binding sites as defined above, and selected the 50 best docking solutions in order to be evaluated. The 50 best docking solutions were ranked according to the best total FlexX scoring function value [20]. The most and least stable docking models from each 50 solutions were recorded for each one of the four binding site models. Additionally, visual inspection was performed for some of the selected docking models.

3. Results

In order to check the accuracy of the FlexX docking program, we have docked the TR natural substrate (TS_2) into the TR binding site. In general, considering the four binding site models, the docking results were not very satisfactory when we analyzed the root mean square deviation values (RMSd) which showed different binding modes and higher values (i.e., RMSd > 3 Å) when compared with the crystallographic structure (**1BZL**). However, when using the **W22** sub-pocket binding site model, TS_2 could be docked with favorable binding energy values, and its energy value was comparable to the most potent peptidomimetic (**18**).

Table 1 shows the 21 compounds docked into the TR active site and their negative logarithm of the minimum concentration that inhibits 50% of the enzyme activity (pIC_{50}). For each compound, 50 docked structures were obtained for the four active site models, except for derivatives **19** and **13**. Considering the **All** binding site model (i.e., system without sub-pocket focusing), compound **19** showed only five docking poses, and considering the **F396′** binding site model, compound **13** did not show any solution. The total score of the highest (*H*) and the lowest (*L*) scored structures for all peptidomimetics in all four binding sites according to the FlexX score function are shown in Table 2.

Analyzing the decreasing order of score docking values of the four binding site models (Table 3), we observed different orders for each binding site models of the TR structure. In order to make our analysis easier, we organized the 21 peptidomimetics in three groups, according to their pIC_{50} potency values (Tables 1 and 3): (i) *higher potency* ($pIC_{50} \geq 4.0$, i.e., compounds **18**, **13**, **7**, and **8**), (ii) *middle potency* ($4.0 > pIC_{50} \geq 3.0$, i.e., compounds **19**, **20**, **17**, **14**, **11**, **2**, **15**, **16**, **1**, **12**, and **5**), and (iii) *lower potency* ($pIC_{50} < 3.0$, i.e., compounds **3**, **9**, **6**, **4**, **21**, and **10**).

Evaluating the energy range score in relation to the highest and the lowest scored structure of each binding site model, we observed the following range values. The **All** binding site model has scoring values ranging from −40 to −18 kcal mol^{-1}; the **W22** binding site model, from −42 to −17 kcal mol^{-1}; the **Y111**, −36 to −19 kcal mol^{-1}; and the **F396′** binding site model, from −41 to

Table 2
The total FlexX score (kcal mol^{-1}) of the highest (*H*) and the lowest (*L*) scored compounds' poses, according to the four binding site models.

#	**All**		**W22**		**Y111**		**F396′**	
	H	*L*	*H*	*L*	*H*	*L*	*H*	*L*
1	−32.195	−19.719	−25.039	−19.745	−23.430	−18.526	−26.920	−20.290
2	−24.597	−21.122	−25.941	−20.126	−20.602	−11.565	−26.100	−23.310
3	−30.247	−22.603	−27.395	−22.064	−29.362	−22.281	−28.850	−23.840
4	−31.335	−25.286	−25.855	−20.879	−33.154	−23.081	−30.99	−20.390
5	−27.439	−22.285	−23.775	−20.254	−19.795	−16.924	−26.98	−23.280
6	−21.582	−14.956	−16.653	−11.206	−22.553	−6.940	−24.50	−10.590
7	−33.680	−26.471	−34.994	−22.022	−33.313	−25.632	−29.52	−24.710
8	−32.227	−26.935	−37.384	−30.711	−29.201	−15.106	−29.89	−20.850
9	−30.446	−24.879	−29.524	−24.903	−23.902	−20.089	−33.10	−28.420
10	−34.348	−28.042	−27.076	−25.475	−31.795	−25.081	−39.46	−33.020
11	−34.859	−31.039	−37.889	−30.756	−27.145	−20.356	−39.52	−34.420
12	−36.332	−24.567	−30.304	−22.416	−27.754	−20.565	−34.92	−24.330
13	−26.952	−23.515	−22.451	−19.768	−35.725	−26.291	nd	nd
14	−27.429	−25.783	−31.618	−28.048	−19.355	−9.180	−38.610	−36.850
15	−27.490	−26.599	−33.025	−20.006	−22.156	−16.605	−12.860	−10.000
16	−25.072	−22.847	−41.915	−37.360	−21.145	−18.701	−17.390	−15.390
17	−39.911	−30.343	−37.218	−28.084	−28.561	−23.208	−41.030	−33.970
18	−35.253	−27.934	−31.320	−25.593	−35.817	−28.215	−25.370	−21.890
19	−17.816	−14.046	−37.094	−32.790	−25.931	−19.283	−27.000	−24.970
20	−30.866	−18.907	−28.667	−16.796	−32.871	−29.215	−23.670	−21.340
21	−28.887	−25.344	−34.439	−29.051	−23.565	−22.282	−27.120	−24.180

nd = not determined.

Table 3
Potency (pIC_{50}) and FlexX ranked orders of the compounds, according to the four binding site models.

#	pIC_{50}	**All** model		**W22** model		**Y111** model		**F396′** model	
		Order	Score	Order	Score	Order	Score	Order	Score
18	4.98	**17**	−40	**16**	−42	**18**	−36	**17**	−41
13	4.93	**12**	−36	**11**	−38	**13**	−36	**11**	−40
7	4.41	**18**	−35	**8**	−37	**7**	−33	**10**	−39
8	4.22	**11**	−35	**17**	−37	**4**	−33	**14**	−39
19	3.62	**10**	−34	**19**	−37	**20**	−33	**12**	−35
20	3.61	**7**	−34	**7**	−35	**10**	−32	**9**	−33
17	3.53	**8**	−32	**21**	−34	**3**	−29	**4**	−31
14	3.45	**1**	−32	**15**	−33	**8**	−29	**8**	−30
2	3.40	**4**	−31	**14**	−32	**17**	−29	**7**	−30
11	3.40	**20**	−31	**18**	−31	**12**	−28	**3**	−29
15	3.38	**9**	−30	**12**	−30	**11**	−27	**21**	−27
16	3.29	**3**	−30	**9**	−30	**19**	−26	**19**	−27
12	3.26	**21**	−29	**20**	−29	**9**	−24	**5**	−27
1	3.26	**15**	−27	**3**	−27	**21**	−24	**1**	−27
5	3.09	**5**	−27	**10**	−27	**1**	−23	**2**	−26
3	2.82	**14**	−27	**2**	−26	**6**	−23	**18**	−25
9	2.76	**13**	−27	**4**	−26	**15**	−22	**6**	−25
4	2.57	**16**	−25	**1**	−25	**16**	−21	**20**	−24
6	2.57	**2**	−25	**5**	−24	**2**	−21	**16**	−17
21	2.56	**6**	−22	**13**	−22	**5**	−20	**15**	−13
10	2.41	**19**	−18	**6**	−17	**14**	−19	**13**	nd

nd = not determined.

−13 kcal mol^{-1} (Table 2). Therefore, we have arbitrarily grouped the 21 compounds according their scoring values for each binding site model as follows: higher score (score ≤ -35 kcal mol^{-1} for **All**, **W22**, and **F396′** binding site models and score ≤ -30 kcal mol^{-1} for **Y111** binding site model), lower score (score ≥ -25 kcal mol^{-1} for **All**, **W22** and **F396′** binding site models and score ≥ -20 kcal mol^{-1} for **Y111** binding site model), and the remaining scores in middle score group.

The docking results of the **All** binding site model, shown in Table 3, show the most potent compound, **18**, at the third ranked position, but it has, at least, correctly classified it into the higher score group. Furthermore, compound **6** (*lower potency* group) was also correctly classified in the lower score group.

Considering the **W22** model (Table 3), compounds **8** and **7** (*higher potency* group) were correctly classified in the higher score group, however, compound **13** (*high potency*) was incorrectly classified in the lower score group, the same group of compound **6** (*lower potency* group), which was, however, correctly classified.

Taking into account the **Y111** model, three compounds (**18**, **13**, and, **7**) of the *higher potency* group were ranked by FlexX program in the correct order of potency, which means a 75% success rate for these compounds, and also they were correctly classified in the higher score group. Compound **10** (*lower potency* group), however, was incorrectly classified in the higher score group.

Considering the **F396′** model, the two most potent compounds had the worst behavior in this case: peptidomimetic **18** was classified in the lower score group and **13** was not docked at all. Moreover, the least potent compound, compound **10**, was incorrectly classified in the higher score group, being ranked in the third position.

According to these results, the binding site model that best reproduces the observed order of potency of the 21 peptidomimetics is the one using sub-pocket **Y111**.

4. Discussion

In this work we have docked the Trypanothione Reductase (TR) natural substrate (trypanothione, TS_2) and a series of 21 peptidomimetics into the TR active site using the FlexX program. Four enzyme binding site models were considered, namely **All**, **W22**, **Y111**, and **F396′**. According to our results, there is a variation in ranking orders of peptidomimetics depending on the binding site model used.

The FlexX docking results for the substrate (TS_2) show no poses having the same binding mode when compared with the crystallographic data revealed by root mean square deviation values between the reference structure and the best-energy structures are very considerable (RMSd $>$ 3 Å). This is probably due to the higher degree of conformational freedom [22] and the almost symmetrical structure of TS_2 [17]. However, in all the 50 poses, the TS_2 structures were docked inside the binding site, as in the **W22** model, where the binding energy values were comparable to the most potent peptidomimetics (**18**). Additionally, Fig. 1 shows two different poses of TS_2 (the highest and the lowest scored ones) docked into the TR binding site and the reference crystallographic binding mode.

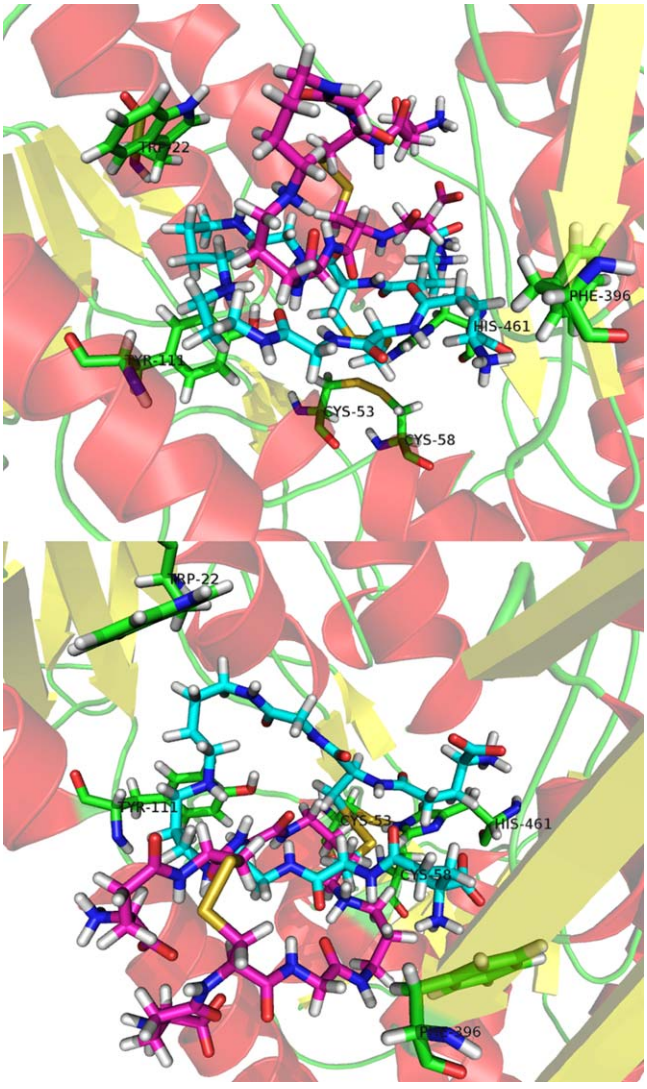

Fig. 1. FlexX docking poses of trypanothione disulfide (TS_2) into Trypanothione Reductase (TR) binding site in **All** model. Some catalytic residues are shown as green sticks (Trp22, Cys53, Cys58, Tyr111, Phe396′, and Hys461′) and the crystallographic structure of TS_2 is colored in blue. In the figure above the TS_2 best ranked structure is colored in pink. In the figure below the TS_2 worst ranked structure is colored in pink.

The 4-methoxy-β-naphtylamide derivatives **12** (pIC_{50} = 3.26 M) and **5** (pIC_{50} = 3.09 M) are structurally related to each other, since the Lys and benzyloxycarbonyl groups of **5** are replaced in **12** by Arg and Phe-Pro residues, respectively (Table 1). Both belongs to the *middle potency* group (see Section 3 for this definition) and the FlexX score function was able to discriminate between these two compounds, and it has reproduced the same potency order in all binding site models, although the compounds **12** and **5** have showed more variation in their scoring values in all models (Table 3).

Analyzing the most potent 4-methoxy-β-naphtylamide derivatives, compounds **18** and **7** (Table 1), we see that by the increase of the peptidomimetic chain with just one single amino acid residue (compound **18** has an Ala residue), the FlexX score function was able to discriminate between these two structurally related compounds, although it does not always reproduce the same potency order in all binding site models (Table 3). The **Y111** model was the best model in predicting the potency order for these compounds, followed by the **All** model, while the other two models (i.e., **W22** and **F396′**) reversed the potency order.

Analyzing the results for the *higher potent* compounds shown in Table 3, e.g., derivatives **18**, **13**, and **7**, the best results were obtained for the **Y111** model, in which the same order of potency was achieved. The other three binding site models (i.e., **All**, **W22**, and **F396′**) did not reproduce the experimental results as a whole, and in some cases, they reversed the order of potency: compound **13** was classified in the *lower score* group in two of the three binding site models (i.e., **All** and **W22**), and in one of them (i.e., **F396′**), it could not even be docked at all. Fig. 2 shows the most potent and better ranked compounds, **13** and **18**, according to the **Y111** model.

Analyzing the results for non-substituted β-naphtylamide analog (compound **3** at Table 1) in the better model (**Y111**), we see that it was ranked in inverse order of biological potency (Table 3). This could be explained by the default FlexX scoring function [20,24], which puts an additional weight on charged hydrogen bonds (included in the ΔG_{match} equation term) by a factor of 1.667 per charged hydrogen bond partner resulting that the partial charge of participating ligand atom is above a given threshold [24]. As shown in Table 3, only the **Y111** model was not

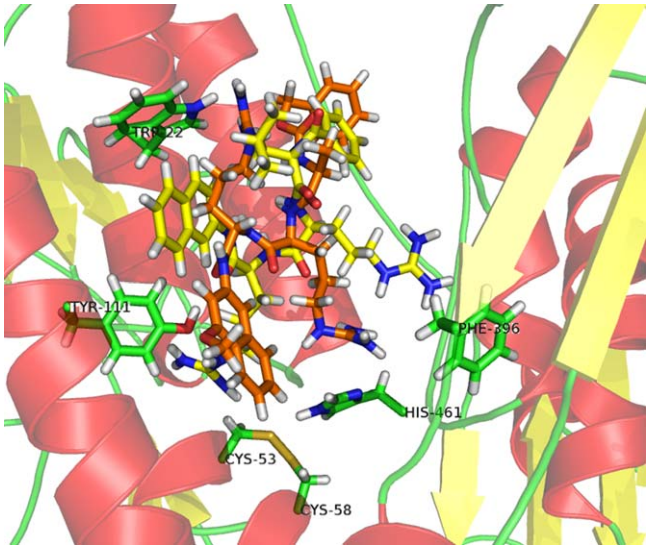

Fig. 2. FlexX docking poses of the best ranked structures of compounds **13** (yellow) and **18** (orange) into TR binding site in **Y111** model. Some catalytic residues are shown as green sticks (Trp22, Cys53, Cys58, Tyr111, Phe396′, and Hys461′).

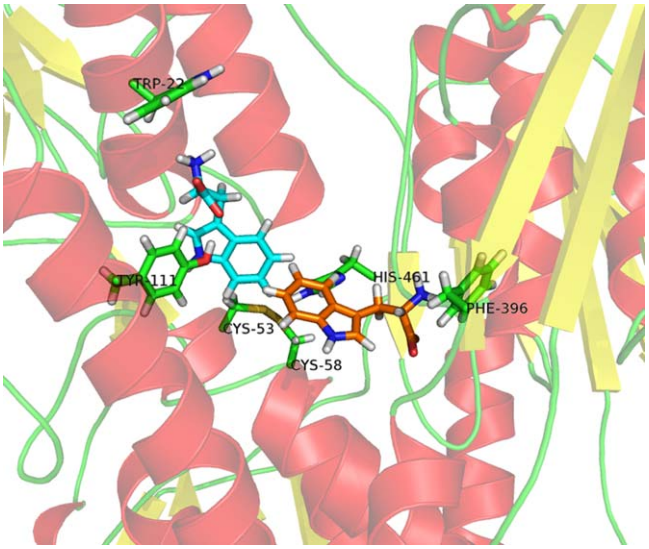

Fig. 3. FlexX docking poses of compound **6** (a single tryptophan residue) into TR binding site in **All** model. Some catalytic residues are shown as green sticks (Trp22, Cys53, Cys58, Tyr111, Phe396′, and Hys461′). The best (colored in blue) and the worst (colored in orange) ranked structures of derivative **6** are shown.

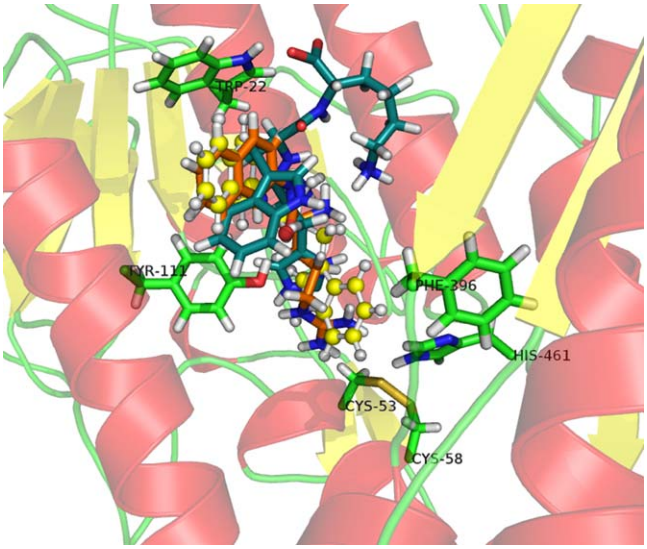

Fig. 4. Flex docking poses of the best ranked structures of compounds **3** (orange), **4** (yellow ball-stick), and **10** (dark green) into TR binding site in *Y111* model. Some catalytic residues are shown as green sticks (Trp22, Cys53, Cys58, Tyr111, Phe396′, and Hys461′).

able to reproduce the compound **3** experimental order due to this additional weight.

The FlexX function scores the "Tryptophan derivatives" (i.e., compounds **9**, **6**, and **10**, Table 1), inverting their potency order (Table 3). It is also included in the ΔG_{match} term (as discussed above) and the explanation is based on the penalty function for ionic interactions, in which the more basic charged residues are present, the better the compound will be ranked [20,24]. Since histidine residue is less basic than Lys (pK_a = 6.04 and 10.54, respectively), this justifies the obtained ranking order in the different models (Table 3).

In some cases, compound **6** was positioned at many different location sites in all models due to the particularities of FlexX base fragmentation [25,26] since its structure corresponds to a single tryptophan residue (Table 1). Fig. 3 shows some uncharacteristic positions for compound **6** in the TR site. In all models, excluding **Y111**, compound **6** (from the *lower potency* group) was correctly classified in the *lower score* group according to its total FlexX score value. In the model that better reproduces the biological potency order, the **Y111** model, compound **6** was erroneously classified in the *middle score* group.

Other two *lower potency* compounds, **3** and **4**, despite of sharing some similarities (structures and potency, Table 1) their score values were super estimated in all models (Table 3). No one was classified in the lower score group and only **W22** model was able to reproduce the experimental order (Table 3). In the best model (**Y111**), the FlexX base fragmentation algorithm [25,26] selected the aromatic moiety to be better ranked than the other pattern groups. As an example, compounds **4** and **10**, which have the aromatic residue tryptophan, are better scored than **3**. This is due to the lipophilic score contribution calculated by FlexX scoring function that was significantly different for these compounds (Lipo score for **4** = −10.83; **10** = −8.34; and **3** = −7.65). Fig. 4 shows the similarity location of the peptides **3**, **4**, and **10** in **Y111** model.

Considering the molecular volume, the FlexX scoring function was able to deal adequately with the bulkiest derivative, compound **16**, which has a molecular volume (MV) of 2 030 Å^3. In all four models, this compound was correctly ranked in the *middle potency* class, in spite of previous published limitations in FlexX methodology [20,23,24]. Interestingly, FlexX could not correctly rank compounds **19** (MV = 1 956 Å^3, the second bulkier), in the **All** model, and **13** (1 912 Å, the third bulkier), in the **F396′** model. The reason for this behavior should be due to the FlexX penalty applied to the number of rotatable bonds. Analyzing the single residue (arginine or tryptophan) linked to β-naphtylamide moiety in compounds **3** and **4**, respectively, the FlexX penalized the guanidine derivative due to its higher number of rotational bonds compared to the imidazole derivative. When measuring the ligand conformational entropy (Rot score for **3** = 7.00 and **4** = 4.20), the potency order (Tables 1 and 3) is reversed in **All**, **Y111** and **F396′**. These results for compounds **3** and **4** could justify the absence of results for **19** and **13** in two diverse docking runs and were pointed by the authors in the score function development [20].

After achieving the model that best reproduces the biological potency order (**Y111**), we compared our results with a previous published one [11]. These authors reported that compound **18** is directly bind into TR active site, pointing the benzyloxycarbonyl group to the "Z-site" (region near the F396′ residue) [27] and the 4-methoxy-β-naphtylamide group towards the W22 and M114 residues. In our 50 best ranked poses (**Y111** model), **18** do not show this overall orientation (Fig. 2).

When only one of the four models adequately describes the potency order, this apparently could represent a drawback in FlexX methodology [20,23] but looking towards the drug screening of the inhibitors for Chagas disease it is important to have a fast and accurate model to screen the new series of the potent chemical compounds in development against Trypanothione Reductase.

5. Conclusions

The binding site **Y111** model, using the sub-pocket focusing method, was selected as the best model, since it was able to correctly rank the higher potency group of compounds, showing a 75% success rate. This model could be used to study new peptidomimetics inhibitors of *T. cruzi* Trypanothione Reductase (TR), pointing to possible new lead compounds for the treatment of Chagas' disease.

The **W22** residue which was assigned as a part of the hydrophobic wall into the TR enzyme [11] and the **F396′** that forms the "Z-site" [11,27] was pointed out as the main residues for the interaction with these inhibitors. Our calculations using these residues into the sub-pockets of the enzyme and the **All** models

(definition in Section 2) presented some results that reversed the potency order of some derivatives (Table 3), which reinforce the meaning of the model with tyrosine in reproducing the biological assay.

In spite of the great encouragement provided by FlexX in the docking protocol, one should be aware of the limitations of this method: i.e., the protein is treated as a "rigid-body" approach and the correct placement of the ligand anchor fragment is problematical.

This docking model using tyrosine residue focusing site should be applied in a future step of the drug discovery road when selecting the active compounds against Trypanothione Reductase independently of the chemical class of the series.

Acknowledgments

This work was performed by the Chagas' Disease Research Group of LabMMol which is funded by CAPES, CNPq and FAPERJ, to whom the authors are grateful for financial support.

References

[1] J.R. Coura, S.L. de Castro, A critical review on Chagas' disease chemotherapy, Mem. Inst. Oswaldo Cruz 97 (2002) 3–24.
[2] J.A. Urbina, R. do Campo, Specific chemotherapy of Chagas disease controversies and advances, Trends Parasitol. 19 (2003) 495–501.
[3] A.H. Fairlamb, P. Ulrich, B.T. Chait, A. Cerami, Trypanothione A novel bis (glutathionyl) spermidine cofactor for glutathione reductase in trypanosomatids, Science 227 (1985) 1485–1487.
[4] A.H. Fairlamb, A. Cerami, Metabolism and functions of trypanothione in the *Kinetoplastida*, Ann. Rev. Microbiol. 46 (1992) 695–729.
[5] C.H. Faerman, S. Savvides, C. Strickland, Charge is the major discriminating factor for glutathione reductase versus trypanothione reductase inhibitors, Bioorg. Med. Chem. 4 (1996) 1247–1253.
[6] R.L. Krauth-Siegel, R. Schoneck, Trypanothione reductase and lipoamide dehydrogenase as target for a structure-based drug design, FASEB J. 9 (1995) 1138–1146.
[7] R.H. Schirmer, J.G. Müller, R.L. Krauth-Siegel, Disulfide-reductase inhibitors as chemotherapeutical agents the design of drugs for trypanosomiasis and malaria, Angew. Chem. Int. Ed. Engl. 34 (1995) 141–154.
[8] A.T. Evans, S.L. Croft, Antileishmanial actions of tricyclic neuroleptics appear to lack structural specificity, Biochem. Pharmacol. 48 (1994) 613–616.
[9] S. Girault, E. Davioud-Charvet, L. Salmon, A. Berecibar, M.A. Debreu, C. Sergheraert, Structure–activity relationships in 2-aminodiphenylsulfides against trypanothione reductase from *Trypanosoma cruzi*, Bioorg. Med. Chem. 8 (1998) 1175–1180.
[10] K. Blumenstiel, R. Schöneck, V. Yardley, S.L. Croft, R.L. Krauth-Siegel, Nitrofuran drugs as common subversive substrates of *Trypanosoma cruzi* lipoamide dehydrogenase and trypanothione reductase, Biochem. Pharmacol. 58 (1999) 1791–1799.
[11] J.H. Mc Kie, J. Garforth, R. Jaouhari, C. Chan, H. Yin, T. Besheya, A.H. Fairlamb, K.T. Douglas, Specific peptide inhibitors of trypanothione reductase with backbone structures unrelated to that of substrate potential rational drug design lead frameworks, Amino Acids 20 (2001) 145–153.
[12] M. Paulino, F. Iribarne, M. Dubin, S. Aguilera-Morales, O. Tapia, A.O. Stoppani, The chemotherapy of Chagas' disease: an overview, Mini Rev. Med. Chem. 5 (2005) 499–519.
[13] C. Dumas, M. Oullette, J. Tovar, M.L. Cunningham, A.H. Fairlamb, S. Tamar, M. Olivier, B. Papadoupoulou, Disruption of the trypanothione reductase gene of Leishmania decreases its ability to survive oxidative stress in macrophages, EMBO J. 15 (1997) 2590–2598.
[14] J. Tovar, S. Wilkinson, J.C. Mottran, A.H. Fairlamb, Evidence that trypanothione reductase is an essential enzyme in *Leishmania* by targeted replacement of the tryA gene locus, Mol. Microbiol. 29 (1998) 653–660.
[15] R.L. Krauth-Siegel, G.H. Coombs, Enzymes of parasite thiol metabolism as drug targets, Parasitol. Today 15 (1999) 404–409.
[16] S. Krieger, W. Schwarz, M.R. Ariyanayagam, A.H. Fairlamb, R.L. Krauth-Siegel, C. Clayton, Trypanosomes lacking trypanothione reductase are avirulent and show increased sensitivity to oxidative stress, Mol. Microbiol. 35 (2000) 542–552.
[17] C.H. Bond, Y. Zhang, M. Berriman, M.L. Cunningham, A.H. Fairlamb, W.N. Hunter, Crystal structure of *Trypanosoma cruzi* trypanothione reductase, and the structure based discovery of natural product inhibitors, Structure 7 (1999) 81–89.
[18] H.M. Berman, J. Westbrook, Z. Feng, G. Gilliland, T.N. Bhat, H. Weissig, I.N. Shindyalov, P.E. Bourne, The Protein Data Bank, Nucleic Acids Res. 28 (2000) 235–242.
[19] SYBYL, Version 7.0, Tripos Inc., St. Louis, Missouri.
[20] M. Rarey, B. Kramer, T. Lengauer, G. Klebe, A fast flexible docking method using an incremental construction algorithm, J. Mol. Biol. 261 (1996) 470–489.
[21] P.L. Privalov, S.J. Gill, Ability of protein structure and hydrophobic interaction, in: C.B. Anfinsen (Ed.), Adv. Protein Chem., vol. 39, Academic Press Inc., San Diego, 1989, pp. 191–231.
[22] G.B. Henderson, J. Glushka, D. Cowburn, A. Cerami, Synthesis and NMR characterization of the trypanosomatid metabolite, N1,N8-bis(glutathionyl)spermidine disulphide (trypanothione disulphide), J. Chem. Soc. Perkin Trans. 1 (1990) 911–914.
[23] M. Rarey, B. Kramer, T. Lengauer, The particle concept placing discrete water molecules during protein–ligand docking predictions, Proteins 34 (1999) 17–28.
[24] M. Stahl, M. Rarey, Detailed analysis of scoring functions for virtual screening, J. Med. Chem. 44 (2001) 1035–1042.
[25] M. Rarey, B. Kramer, T. Lengauer, Multiple automatic base selection protein–ligand docking based on incremental construction without manual intervention, J. Comput. Aided Mol. Des. 11 (1997) 369–384.
[26] M. Rarey, B. Kramer, T. Lengauer, Placement of medium-sized molecular fragments into active sites of proteins, J. Comput. Aided Mol. Des. 10 (1996) 41–54.
[27] C. Chan, H. Yin, J. Garforth, J.H. Mc Kie, R. Jaouhari, P. Speers, K.T. Douglas, P.J. Rock, V. Yardley, S.L. Croft, A.H. Fairlamb, Phenothiazine Inhibitors of trypanothione reductase as potential antitrypanosomal and antileishmanial drugs, J. Med. Chem. 41 (1998) 148–156.